



Probing Wilson loops in $\mathcal{N} = 4$ Chern–Simons–matter theories at weak coupling



Luca Griguolo^a, Matias Leoni^b, Andrea Mauri^c, Silvia Penati^{c,d}, Domenico Seminara^e

^a Dipartimento di Fisica e Scienze della Terra, Università di Parma and INFN, Gruppo Collegato di Parma, Viale G.P. Usberti 7/A, 43100 Parma, Italy

^b Physics Department, FCEyN-UBA & IFIBA-CONICET Ciudad Universitaria, Pabellón I, 1428 Buenos Aires, Argentina

^c Dipartimento di Fisica dell'Università degli studi di Milano-Bicocca, Piazza della Scienza 3, I-20126 Milano, Italy

^d INFN Sezione di Milano-Bicocca, Piazza della Scienza 3, I-20126 Milano, Italy

^e Dipartimento di Fisica, Università di Firenze and INFN Sezione di Firenze, via G. Sansone 1, 50019 Sesto Fiorentino, Italy

ARTICLE INFO

Article history:

Received 17 November 2015

Accepted 7 December 2015

Available online 23 December 2015

Editor: N. Lambert

ABSTRACT

For three-dimensional $\mathcal{N} = 4$ super-Chern–Simons–matter theories associated to necklace quivers $U(N_0) \times U(N_1) \times \dots \times U(N_{2r-1})$, we study at quantum level the two kinds of $1/2$ BPS Wilson loop operators recently introduced in [arXiv:1506.07614](https://arxiv.org/abs/1506.07614). We perform a two-loop evaluation and find the same result for the two kinds of operators, so moving to higher loops a possible quantum uplift of the classical degeneracy. We also compute the $1/4$ BPS bosonic Wilson loop and discuss the quantum version of the cohomological equivalence between fermionic and bosonic Wilson loops. We compare the perturbative result with the Matrix Model prediction and find perfect matching, after identification and remotion of a suitable framing factor. Finally, we discuss the potential appearance of three-loop contributions that might break the classical degeneracy and briefly analyze possible implications on the BPS nature of these operators.

© 2015 The Authors. Published by Elsevier B.V. This is an open access article under the CC BY license (<http://creativecommons.org/licenses/by/4.0/>). Funded by SCOAP³.

1. Introduction

One of the most interesting classes of observables in supersymmetric gauge theories is constituted by BPS Wilson loops [1,2]. They provide an exciting arena where exact computations can be performed through localization techniques [3], so interpolating non-trivially between weak and strong coupling regimes.

The first and most famous example is the $1/2$ BPS circular Wilson loop, originally constructed in $\mathcal{N} = 4$ super-Yang–Mills theory. It is calculated by a simple Gaussian matrix model and reproduced at strong coupling through the AdS/CFT correspondence [1,2]. The original proposal has been generalized to less supersymmetric loops [4] and in theories with $\mathcal{N} = 2$ supersymmetry [3]. In all these constructions the key point is to improve the holonomy of the gauge connection by coupling some of the scalar fields to the appropriate contours. The resulting operators are BPS and their expectation values can be computed by adding a suitable Q-exact

term to the classical action, so that the relevant path-integral is semiclassically exact [3].

In three dimensions the story is a little bit different. $\mathcal{N} = 2$ Chern–Simons theories still possess circular $1/2$ BPS Wilson loops obtained through scalar couplings, which are calculated by localization techniques [5]. Going to more supersymmetric theories, as the $\mathcal{N} = 6$ ABJ(M) model, the construction of $1/2$ BPS operators has to be refined [6] (see also [7] for a generalization to other contours). In fact, scalar couplings only provide $1/6$ BPS Wilson loops and fermionic couplings have to be invoked to enhance supersymmetry. More surprisingly, $1/2$ BPS Wilson loops in ABJ(M) theory are seen equivalent to a linear combination of $1/6$ BPS ones [6,8]. In fact, they belong to the same cohomology class of the localizing supercharge and thus, up to framing anomalies, they are the same observable at quantum level. This phenomenon is a three-dimensional novelty, that has been checked concretely in perturbation theory [13,14] and certainly needs a more profound investigation. Recently, the construction of $1/2$ BPS Wilson loops has been presented [9,10] in $\mathcal{N} = 4$ quiver Chern–Simons theories [11,12]. In the case of circular and linear quivers with non-vanishing CS levels, two apparently independent $1/2$ BPS circular loops emerge, which share the same supersymmetry and belong to the same cohomology class of the familiar bosonic $1/4$ Wilson

E-mail addresses: luca.griguolo@pr.infn.it (L. Griguolo), leoni@df.uba.ar (M. Leoni), andrea.mauri1@unimib.it (A. Mauri), silvia.penati@mib.infn.it (S. Penati), domenico.seminara@fi.infn.it (D. Seminara).

loop operator. These properties have been derived at classical level and should be checked against truly quantum computations, where divergences and/or anomalies could arise, possibly lifting the classical degeneracy.

In this paper we perform explicitly a perturbative computation of the two fermionic Wilson loops at second order in the coupling constant, finding perfect consistency with the classical picture and no lifting of the quantum expectation value. At the same order we check the matrix model result obtained from the localization procedure and, consequently, confirm the cohomological equivalence with the 1/4 BPS loop. The plan of our Letter is the following. In Section 2 we briefly recall the construction of the Wilson loop operators in $\mathcal{N} = 4$ circular Chern–Simons quivers. Section 3 is devoted to the perturbative computation of the expectation value of the relevant Wilson loop operators. In Section 4 we check their cohomological equivalence at quantum level. Matrix model results are explicitly seen to be consistent with our quantum calculations in Section 5. A critical analysis of the degeneracy problem is presented in Section 6, where we discuss the potential appearance of higher-order contributions that might turn out to be different for the two fermionic Wilson loops.

2. Circular BPS Wilson loops in $\mathcal{N} = 4$ CS-matter theories

We consider a Chern–Simons-matter theory associated to a circular quiver with gauge group $U(N_0) \times U(N_1) \times \dots \times U(N_{2r-1})$ ($N_{2r} \equiv N_0$). Besides the gauge sector containing vectors $A_{(A)}^\mu$ in the adjoint representation of the group $U(N_A)$, the theory contains matter scalars $(q_{(2A+1)}^I)^j_j$ ($(\bar{q}_{(2A+1)I})^{\hat{j}}_{\hat{j}}$) in the (anti)bifundamental representation of the $U(N_{2A+1})$, $U(N_{2A+2})$ nodes (indices j and \hat{j} , respectively) and in the fundamental of the R-symmetry $SU(2)_L$ ($I = 1, 2$), twisted scalars $(q_{(2A)}^{\hat{I}})^j_j$ ($(\bar{q}_{(2A)I})^{\hat{j}}_{\hat{j}}$) in the (anti)bifundamental representation of $U(N_{2A})$, $U(N_{2A+1})$ nodes and in the fundamental of the R-symmetry $SU(2)_R$ ($\hat{I} = 1, 2$), plus the corresponding fermions $(\psi_{(2A+1)I})^j_j$ ($(\bar{\psi}_{(2A+1)I}^{\hat{j}})^{\hat{j}}_{\hat{j}}$) and $(\psi_{(2A)I})^{\hat{j}}_{\hat{j}}$ ($(\bar{\psi}_{(2A)I}^I)^j_j$), respectively.

In three-dimensional euclidean space the classical action reads

$$S = \sum_{A=0}^{2r-1} (S_{CS}^{(A)} + S_{mat}^{(A)}) + S_{pot} + S_{gf} \quad (1)$$

where

$$S_{CS}^{(A)} = -\frac{i}{2} k_A \int d^3x \varepsilon^{\mu\nu\rho} \text{Tr} \left(A_{(A)\mu} \partial_\nu A_{(A)\rho} + \frac{2}{3} i A_{(A)\mu} A_{(A)\nu} A_{(A)\rho} \right) \quad (2)$$

$$S_{mat}^{(A)} = \int d^3x \text{Tr} \left[D_\mu q_{(A)} D^\mu \bar{q}_{(A)} + i \bar{\psi}_{(A)} \gamma^\mu D_\mu \psi_{(A)} \right]$$

while S_{gf} is the gauge-fixing plus ghost action and S_{pot} the matter interaction action, whose explicit expression can be found for instance in [18]. This part of the action does not enter two-loop diagrams, so we will ignore it in the rest of the paper.

$\mathcal{N} = 4$ supersymmetry requires the CS levels to satisfy

$$k_A = \frac{k}{2} (s_A - s_{A-1}), \quad s_A = \pm 1, \quad k > 0 \quad (3)$$

We will consider the case $s_A = (-1)^{A+1}$, which leads to alternating $\mp k$ levels.

In [9,10] Wilson loop operators (WL) have been introduced that are classically BPS. These are defined locally for each site of the

quiver and involve at most three adjacent nodes. Therefore, restricting for simplicity to node $U(N_1)$ and its nearest-neighbor $U(N_0)$ and $U(N_2)$ we will consider the following loop operators integrated on the unit circle Γ ($x^\mu = (\cos \tau, \sin \tau, 0)$, $\tau \in [0, 2\pi]$):

Fermionic 1/2 BPS ψ_1 -Wilson loop. When referred to node $U(N_1)$ it is defined as [10]¹

$$W_{\psi_1}[\Gamma] = \text{Tr} P \exp \left(-i \int_\Gamma d\tau \mathcal{L}_F^{\psi_1}(\tau) \right) \quad (4)$$

where

$$\mathcal{L}_F^{\psi_1} = \begin{pmatrix} \mathcal{A}_{(1)} & \bar{c}_\alpha \psi_{(1)\hat{1}}^\alpha \\ c^\alpha \bar{\psi}_{(1)\alpha}^{\hat{1}} & \mathcal{A}_{(2)} \end{pmatrix} \quad (5)$$

$$\mathcal{A}_{(1)} = \dot{x}^\mu A_{(1)\mu} - \frac{i}{k} \left(q_{(1)}^I \delta_I^J \bar{q}_{(1)J} + \bar{q}_{(0)I} (\sigma_3)^{\hat{I}}_J q_{(0)}^{\hat{J}} \right)$$

$$\mathcal{A}_{(2)} = \dot{x}^\mu A_{(2)\mu} - \frac{i}{k} \left(\bar{q}_{(1)I} \delta_I^J q_{(1)}^J + q_{(2)}^{\hat{I}} (\sigma_3)^{\hat{I}}_{\hat{J}} \bar{q}_{(2)\hat{J}} \right)$$

and the commuting spinors c, \bar{c} are (with $C\bar{c} = -\frac{i}{k}$)

$$c(\tau) = C \left(\cos \frac{\tau}{2} - \sin \frac{\tau}{2}, \cos \frac{\tau}{2} + \sin \frac{\tau}{2} \right)$$

$$\bar{c}(\tau) = \bar{C} \begin{pmatrix} \cos \frac{\tau}{2} - \sin \frac{\tau}{2} \\ \cos \frac{\tau}{2} + \sin \frac{\tau}{2} \end{pmatrix} \quad (6)$$

Fermionic 1/2 BPS ψ_2 -Wilson loop. This loop operator is defined as [10]

$$W_{\psi_2}[\Gamma] = \text{Tr} P \exp \left(-i \int_\Gamma d\tau \mathcal{L}_F^{\psi_2}(\tau) \right) \quad (7)$$

where

$$\mathcal{L}_F^{\psi_2} = \begin{pmatrix} \mathcal{A}_{(1)} & \bar{c}_\alpha \psi_{(1)\hat{2}}^\alpha \\ c^\alpha \bar{\psi}_{(1)\alpha}^{\hat{2}} & \mathcal{A}_{(2)} \end{pmatrix} \quad (8)$$

$$\mathcal{A}_{(1)} = \dot{x}^\mu A_{(1)\mu} - \frac{i}{k} \left(-q_{(1)}^I \delta_I^J \bar{q}_{(1)J} + \bar{q}_{(0)\hat{I}} (\sigma_3)^{\hat{I}}_J q_{(0)}^{\hat{J}} \right)$$

$$\mathcal{A}_{(2)} = \dot{x}^\mu A_{(2)\mu} - \frac{i}{k} \left(-\bar{q}_{(1)I} \delta_I^J q_{(1)}^J + q_{(2)}^{\hat{I}} (\sigma_3)^{\hat{I}}_{\hat{J}} \bar{q}_{(2)\hat{J}} \right)$$

and the commuting spinors c, \bar{c} given by (with $C\bar{c} = \frac{i}{k}$)

$$c(\tau) = -C \left(\cos \frac{\tau}{2} + \sin \frac{\tau}{2}, -\cos \frac{\tau}{2} + \sin \frac{\tau}{2} \right)$$

$$\bar{c}(\tau) = \bar{C} \begin{pmatrix} \cos \frac{\tau}{2} + \sin \frac{\tau}{2} \\ -\cos \frac{\tau}{2} + \sin \frac{\tau}{2} \end{pmatrix} \quad (9)$$

This loop differs from the previous one for the replacement of the identity matrix with minus the identity matrix in the scalar couplings, the replacement $\psi_{(1)}^{\hat{1}} \rightarrow \psi_{(1)}^{\hat{2}}$ in the off-diagonal elements and the choice of different fermion couplings.

Bosonic 1/4 BPS Wilson loop. We will be also interested in bosonic loop operators that respect 1/4 of the original supersymmetries [9, 10]. For sites N_1 and N_2 they are

¹ For simplicity, we define Wilson loops without any normalization factor.

$$W^{(1)}[\Gamma] = \text{Tr } P \exp \left(-i \int_{\Gamma} d\tau \mathcal{L}_B^{(1)}(\tau) \right)$$

$$W^{(2)}[\Gamma] = \text{Tr } P \exp \left(-i \int_{\Gamma} d\tau \mathcal{L}_B^{(2)}(\tau) \right) \quad (10)$$

where

$$\mathcal{L}_B^{(1)} = \dot{x}^\mu A_{(1)\mu} - \frac{i}{k} \left(\bar{q}_{(0)\dot{i}}(\sigma_3)^{\dot{i}}_j q_{(0)}^{\dot{j}} + q_{(1)I}(\sigma_3)_I^J \bar{q}_{(1)J} \right)$$

$$\mathcal{L}_B^{(2)} = \dot{x}^\mu A_{(2)\mu} - \frac{i}{k} \left(\bar{q}_{(1)I}(\sigma_3)^I_J q_{(1)}^J + q_{(2)\dot{i}}(\sigma_3)^{\dot{i}}_j \bar{q}_{(2)\dot{j}} \right)$$

As proved in [9,10] the fermionic Wilson loops are classically equivalent to the bosonic ones,

$$W_{\psi_i} = W^{(1)} + W^{(2)} + Q V_{\psi_i} \quad i = 1, 2 \quad (11)$$

up to a Q -term, where Q is some linear combination of supercharges. If this cohomological equivalence survives at quantum level, localization techniques applied to the bosonic Wilson loops provide an all-order prediction also for the fermionic operators. For the ABJM orbifold case ($N_i \equiv N$ for any i) the corresponding matrix model has been computed in [17].

3. Two-loop evaluation

In this Section, we present the results for the circular 1/2 BPS and 1/4 BPS WL up to two loops. The computation, that requires regularizing UV divergences and evaluating intricate trigonometric integrals, heavily relies on the techniques introduced in [13,14] to which we refer for details.

We use dimensional regularization with dimensional reduction (DRED) to control potentially divergent integrals. They generally converge in the complex half-plane defined by some critical value of the real part of the regularization parameter ϵ . Using techniques described in [13], they can be computed analytically for any complex value of ϵ and turn out to be expressible in terms of hypergeometric functions. Their actual value for $\epsilon \rightarrow 0$ can be then obtained by analytically continuing the hypergeometric functions close to the origin and expanding the result up to finite terms.

At one-loop we have only two contributions associated with the exchange of one gluon and one fermion line, respectively. The vector exchange vanishes because of the planarity of the circular contour that gets contracted with the Levi-Civita tensor. The contribution from the fermion exchange is proportional to

$$\int_0^{2\pi} d\tau_1 \int_0^{\tau_1} d\tau_2 \frac{(c_1 \gamma^\mu \bar{c}_2)(x_1 - x_2)_\mu}{[(x_1 - x_2)^2]^{\frac{3}{2}-\epsilon}} \quad (12)$$

Choosing the set of euclidean gamma matrices $\gamma^\mu = \{\sigma^3, \sigma^1, \sigma^2\}$, and taking into account the explicit expression of fermion couplings (6) we can write

$$(c_i \gamma^\mu \bar{c}_j)(x_i - x_j)_\mu = -\frac{4i}{k} \sin \frac{\tau_1 - \tau_2}{2} \quad (13)$$

Therefore, the integral becomes

$$\int d\tau_{1>2} \frac{1}{[\sin^2 \frac{\tau_{12}}{2}]^{1-\epsilon}} = \frac{2\pi^{3/2} \Gamma(-\frac{1}{2} + \epsilon)}{\Gamma(\epsilon)} \quad (14)$$

and this expression vanishes in 3d. Therefore, we do not have any one-loop contribution to W_{ψ_1} .

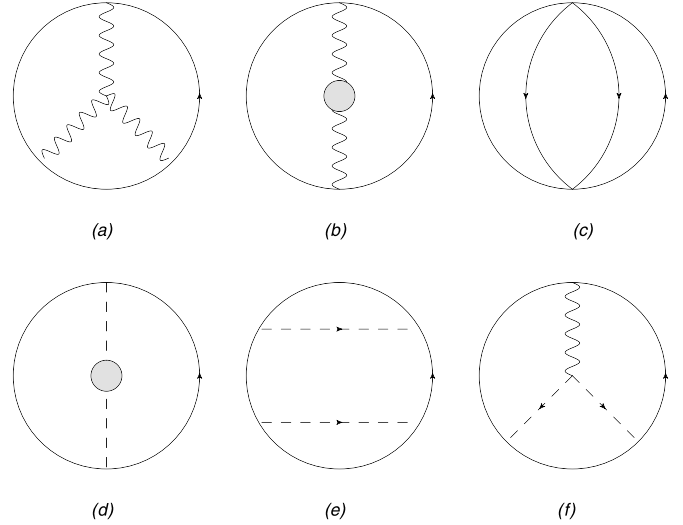


Fig. 1. Non-vanishing two-loop diagrams for ψ_1 and ψ_2 loops. Wavy lines represent gauge propagators, solid lines represent scalars, and dashed lines are fermion propagators. Bubbles represent one-loop corrections to the propagators, as given in Appendix.

We then move to two loops. Contributions that are not trivially vanishing for planarity of the contour are associated to the diagrams in Fig. 1. We list the results for each single diagram, while for details we refer the reader to [13,14].

Diagram (a) – It comes from the gauge part of the third order expansion of the WL contracted with the gauge cubic vertex. Summing the contributions from the two connections $A_{(1)}$ and $A_{(2)}$, we have

$$(a)_{\psi_1} = - \left[N_1(N_1^2 - 1) + N_2(N_2^2 - 1) \right] \frac{1}{k^2} \frac{\Gamma^3(\frac{3}{2} - \epsilon)}{8\pi^{\frac{9}{2}-3\epsilon}} I^{(a)} \quad (15)$$

where

$$I^{(a)} = \int d\tau_{1>2>3} \dot{x}_1^\sigma \dot{x}_2^\eta \dot{x}_3^\zeta \varepsilon^{\xi\tau\kappa} \varepsilon_{\sigma\xi\mu} \varepsilon_{\eta\tau\nu} \varepsilon_{\zeta\kappa\rho} \times \int d^{3-2\epsilon} x \frac{(x-x_1)^\mu (x-x_2)^\nu (x-x_3)^\rho}{|x-x_1|^{3-2\epsilon} |x-x_2|^{3-2\epsilon} |x-x_3|^{3-2\epsilon}} \quad (16)$$

This integral, being finite, can be computed at $\epsilon = 0$ and eventually gives $I^{(a)} = \frac{8}{3}\pi^3$ [13,15]. The final result is then

$$(a)_{\psi_1} = -\frac{1}{24} \frac{N_1(N_1^2 - 1) + N_2(N_2^2 - 1)}{k^2} \quad (17)$$

Diagrams (b) + (c) – Summing the two contributions we obtain

$$[(b) + (c)]_{\psi_1} = \left[N_1^2(N_0 + N_2) + N_2^2(N_1 + N_3) \right] \frac{1}{k^2} \frac{\Gamma^2(\frac{1}{2} - \epsilon)}{8\pi^{3-2\epsilon}} I^{(b+c)} \quad (18)$$

where [15]

$$I^{(b+c)} = \int d\tau_{1>2} \frac{-\dot{x}_1 \cdot \dot{x}_2 + |\dot{x}_1| |\dot{x}_2|}{[(x_1 - x_2)^2]^{1-2\epsilon}} \xrightarrow{\epsilon \rightarrow 0} \pi^2 \quad (19)$$

We then obtain

$$[(b) + (c)]_{\psi_1} = \left[N_1^2(N_0 + N_2) + N_2^2(N_1 + N_3) \right] \frac{1}{8k^2} \quad (20)$$

Diagram (d) – This contribution is proportional to the exchange of a one-loop fermion propagator. Using its explicit expression given in [13] we obtain

$$(d)_{\psi_1} \sim \int d\tau_{1>2} \frac{|\dot{x}_1||\dot{x}_2|}{[(x_1 - x_2)^2]^{1-2\epsilon}} [(c_1\bar{c}_2) - (c_2\bar{c}_1)] \quad (21)$$

where we indicate $c_i \equiv c(\tau_i)$ on the circle. As follows from eq. (6) we have

$$(c_i\bar{c}_j) = -\frac{2i}{k} \cos \frac{\tau_i - \tau_j}{2} \quad (22)$$

so that diagram (d) vanishes identically.

Diagram (e) – Expanding the ψ_1 -loop at fourth order and performing the two possible contractions of fermions we obtain a linear combination of terms of the form

$$\frac{\Gamma^2(\frac{3}{2} - \epsilon)}{4\pi^{3-2\epsilon}} \int d\tau_{1>\dots>4} \frac{(c_i\gamma^\mu\bar{c}_j)(c_k\gamma^\nu\bar{c}_l)(x_i - x_j)_\mu(x_k - x_l)_\nu}{[(x_i - x_j)^2(x_k - x_l)^2]^{\frac{3}{2}-\epsilon}} \quad (23)$$

This expression can be easily elaborated by using identity (13) twice. The contour integrals we are left with are divergent. They can be evaluated away from $\epsilon = 0$ and suitably continued close to the origin (see [13] for details). The result is

$$(e)_{\psi_1} = \frac{3}{8} \frac{N_1^2 N_2 + N_2^2 N_1}{k^2} \quad (24)$$

Diagram (f) – Expanding W_{ψ_1} at third order and contracting with one mixed vertex $\bar{\psi}\psi A$ coming from the action, we obtain the linear combination of six integrals of the form

$$\frac{1}{k} \frac{\Gamma^3(\frac{1}{2} - \epsilon)}{64\pi^{\frac{9}{2}-3\epsilon}} \int d\tau_{1>2>3} (\bar{c}_i\gamma^\xi c_j) \dot{x}_k^\nu \varepsilon_{\nu\mu}{}^\rho \Gamma_{\rho\xi\sigma} \quad (25)$$

where the labels i, j, k run over 1, 2, 3 and

$$\Gamma^{\mu\nu\rho} = \partial_k^\mu \partial_i^\nu \partial_j^\rho \int \frac{d^3x}{[(x - x_1)^2(x - x_2)^2(x - x_3)^2]^{\frac{1}{2}-\epsilon}}$$

The spinorial structure appearing in (25) can be simplified by using standard identities for the product of three Pauli matrices. It is easy to prove that, because of the planarity of the contour the only non-vanishing contributions we are left with are proportional to the bilinears $(c_i\bar{c}_j)$ and $(c_i\gamma^3\bar{c}_j)$. Using identity (22) together with

$$(c_i\gamma^3\bar{c}_j) = \frac{2}{k} \sin \frac{\tau_i - \tau_j}{2}, \quad (26)$$

computing the corresponding color factors and evaluating the integrals using the procedure described in [13] we finally obtain

$$(f)_{\psi_1} = -\frac{1}{2} \frac{N_1^2 N_2 + N_2^2 N_1}{k^2} \quad (27)$$

Summing all the contributions the two-loop result for the ψ_1 -loop is

$$\langle W_{\psi_1}[\Gamma] \rangle|_{2\text{loop}} = (N_1 + N_2) \times \left[1 - \frac{1}{24k^2} \left((N_1^2 + N_2^2 - N_1 N_2 - 1) - 3 \frac{N_0 N_1^2 + N_3 N_2^2}{N_1 + N_2} \right) \right] \quad (28)$$

We now consider the Wilson loop W_{ψ_2} defined in (8), (9). Its perturbative evaluation can be easily performed by exploiting the previous results, where we should take into account that the ψ_2 -loop has slightly different scalar couplings in the \mathcal{A} -terms and different fermionic couplings c, \bar{c} . The fact that the $\psi_{(1)\hat{1}}$ fermion

replaces $\psi_{(1)\hat{1}}$ does not make much difference, as the tree-level propagator for the two fermionic components is the same.

At one loop, the fermion exchange diagram (see equation (12)) involves the bilinear $(c_i\gamma^\mu\bar{c}_j)(x_i - x_j)_\mu$. Computing it with the assignment (9), we obtain the same result (13) up to an overall sign. However, since the diagram is still proportional to integral (14), the ψ_2 -loop contribution at one loop also vanishes in the $\epsilon \rightarrow 0$ limit.

At two loops, non-vanishing contributions are still given in Fig. 1. It is easy to argue that the first three bosonic diagrams give the same result as W_{ψ_1} . In fact, diagram (a) and (b) involve only gauge fields, so they are insensitive to changes in matter couplings. In diagram (c) the matrices (I and σ_3) governing the scalar couplings enter quadratically, so that the sign difference between the two WL definitions does not affect the calculation. Changes in the calculation might be expected from diagrams containing fermions, since a different set of fermionic couplings may give rise to different expressions for the fermionic bilinears $(c_i\bar{c}_j)$ and $(c_i\gamma^\mu\bar{c}_j)$. However, the contribution from diagram (d) is still proportional to expression (21) and vanishes since, as before, $(c_1\bar{c}_2) = (c_2\bar{c}_1)$, as follows immediately from (9). In diagram (e) the double fermion contractions read again as in eq. (23), which involves the bilinear $(c_i\gamma^\mu\bar{c}_j)(x_i - x_j)_\mu$. As we already mentioned, this bilinear has an overall sign compared to the corresponding expression for W_{ψ_1} . However, in (23) the product of two such expressions appears, so that the final result is the same as for W_{ψ_1} . Finally, diagram (f) only involves minimal coupling of fermions to the gauge vectors, which is identical for $\psi_{(1)\hat{1}}$ and $\psi_{(1)\hat{2}}$. Therefore the evaluation of the integrals still depends on the spinorial bilinears $(c_i\bar{c}_j)$ and $(c_i\gamma^3\bar{c}_j)$. Using (9), these can be quickly shown to be identical to the ones for the ψ_1 -loop. Here it is crucial that, due to the planarity of the contour, only the bilinear $(c_i\gamma^\mu\bar{c}_j)$ with $\mu = 3$ enters the calculation. If this were not the case, we would obtain a different result, since for the bilinears along the directions $\mu = 1, 2$ where the circular contour lies there is a sign difference between the two WL.

Summarizing, we find that

$$\langle W_{\psi_1}[\Gamma] \rangle|_{2\text{loop}} = \langle W_{\psi_2}[\Gamma] \rangle|_{2\text{loop}} \quad (29)$$

Therefore, up to this order, there is no quantum uplift of the degeneracy between the two fermionic WL.

Exploiting the previous calculation, it is also immediate to determine the 1/4 bosonic WLs (10). Again, there is no one-loop contribution, while the two-loop ones are given by the first three diagrams in Fig. 1. With suitable adjustments we find ($A = 1, 2$)

$$\frac{\langle W^{(A)} \rangle}{N_A} = 1 - \frac{1}{24k^2} \left[N_A^2 - 3N_{A-1}N_A - 3N_A N_{A+1} - 1 \right] \quad (30)$$

Note that, under identification $N_0 = N_2$ and $N_3 = N_1$, our results (28), (30) coincide with the two-loop expressions for the 1/2 and 1/6 Wilson loops in ABJ, respectively [6,13–15]. Moreover, in the orbifold ABJM $[U(N) \times U(N)]^r$ ($N_A = N$ for all the nodes) the result becomes

$$\begin{aligned} \frac{\langle W_{\psi_1} \rangle}{2N} \Big|_{2\text{loop}} &= \frac{\langle W_{\psi_2} \rangle}{2N} \Big|_{2\text{loop}} \\ &= 1 + \frac{1}{24k^2} (2N^2 + 1) \sim 1 + \frac{1}{12} \left(\frac{N}{k} \right)^2 \\ \frac{\langle W^{(1,2)} \rangle}{N} \Big|_{2\text{loop}} &= 1 + \frac{1}{24k^2} (5N^2 + 1) \sim 1 + \frac{5}{24} \left(\frac{N}{k} \right)^2 \end{aligned} \quad (31)$$

4. Cohomological equivalence at quantum level

It is easy to generalize the results (28) to a generic A site ($A = 0, \dots, 2r-1$) and write

$$\frac{\langle W_{\psi_i}^{(A)} \rangle_{|i=1,2}}{N_A + N_{A+1}} = 1 - \frac{1}{24k^2} \left[N_A^2 + N_{A+1}^2 - N_A N_{A+1} - 1 - 3 \frac{N_{A-1} N_A^2 + N_{A+2} N_{A+1}^2}{N_A + N_{A+1}} \right] + \dots \quad (32)$$

Similarly, generalizing result (30), for bosonic WL related to the A site we have

$$\frac{\langle W^{(A)} \rangle}{N_A} = 1 - \frac{1}{24k^2} \left[N_A^2 - 3N_{A-1}N_A - 3N_A N_{A+1} - 1 \right] + \dots \quad (33)$$

Exploiting these results it is interesting to understand how the classical cohomological equivalence (11) gets enhanced at quantum level. In fact, comparing the previous expressions one can easily realize that the following identity holds

$$\langle W_{\psi_i}^{(A)} \rangle_0 = e^{-i \frac{\ell_A}{2k} (N_A - N_{A+1})} \times \left[e^{i \frac{\ell_A}{2k} N_A} \langle W^{(A)} \rangle_0 + e^{-i \frac{\ell_A}{2k} N_{A+1}} \langle W^{(A+1)} \rangle_0 \right] \quad (34)$$

where $\ell_A = (-1)^{A+1}$ and the subscript “0” means perturbative result (framing zero). Therefore, if we define “framing-one” quantities

$$\begin{aligned} \langle W_{\psi_i}^{(A)} \rangle_1 &= e^{i \frac{\ell_A}{2k} (N_A - N_{A+1})} \langle W_{\psi_i}^{(A)} \rangle_0 \quad j = 1, 2 \\ \langle W^{(A)} \rangle_1 &= e^{-i \frac{\ell_A}{2k} N_A} \langle W^{(A)} \rangle_0 \end{aligned} \quad (35)$$

the previous identity can be rewritten as

$$\langle W_{\psi_i}^{(A)} \rangle_1 = \langle W^{(A)} \rangle_1 + \langle W^{(A+1)} \rangle_1 \quad (36)$$

and looks exactly like the classical relation (11).

5. Matrix model result at weak coupling

We now discuss the matrix model for the necklace quiver theory described in Section 2. The putative matrix integral, which yields the partition function, can be easily obtained by combining the basic building blocks given in [5]. We find [16]

$$\mathcal{Z} = \mathcal{N} \int \prod_{B,i} d\lambda_{Bi} e^{2ik\ell_B \lambda_{Bi}^2} \prod_{B=0}^{2r-1} \frac{\prod_{i<j} \sinh^2(\lambda_{Bi} - \lambda_{Bj})}{\prod_{i,j} \cosh(\lambda_{Bi} - \lambda_{B+1,j})} \quad (37)$$

The constant \mathcal{N} is an overall normalization, whose explicit form is irrelevant in our computation.

In the matrix model language the 1/2 BPS Wilson loop is not a fundamental object, as it can be computed from the 1/4 BPS Wilson loop through the cohomological relation (36). Therefore we focus on the latter. It is given by the vacuum expectation value of the following matrix observable

$$\begin{aligned} W^{(A)} &= \sum_{i=1}^{N_A} e^{2\lambda_{Ai}} = N_A + 2\text{Tr}(\Lambda_A) + 2\text{Tr}(\Lambda_A^2) + \\ &+ \frac{4}{3}\text{Tr}(\Lambda_A^3) + \frac{2}{3}\text{Tr}(\Lambda_A^4) + O(\Lambda_A^5) \end{aligned} \quad (38)$$

where we have introduced the diagonal matrix $\Lambda_A \equiv \text{diag}(\lambda_{A1}, \dots, \lambda_{AN_A})$ for future convenience. In the r.h.s. of (38) we can actually neglect all the odd powers in Λ_A since their expectation value

vanishes at all order in $\frac{1}{k}$ due to the symmetry property of the integrand in (37) under the parity transformation $\lambda_{Ai} \rightarrow -\lambda_{Ai}$.

In order to construct the perturbative series for $W^{(A)}$, first we rescale the eigenvalues λ_{Ai} with $\frac{1}{\sqrt{k}}$. Therefore, the measure factor for large k reads

$$\begin{aligned} &\prod_{B=0}^{2r-1} \frac{\prod_{i<j} \sinh^2 \frac{\lambda_{Bi} - \lambda_{Bj}}{\sqrt{k}}}{\prod_{i,j} \cosh \frac{\lambda_{Bi} - \lambda_{B+1,j}}{\sqrt{k}}} = \\ &\left[1 + \frac{1}{k} \sum_{B=0}^{2r-1} P_B + O\left(\frac{1}{k^2}\right) \right] \prod_{B=0}^{2r-1} \prod_{i<j} \frac{(\lambda_{Bi} - \lambda_{Bj})^2}{k} \end{aligned} \quad (39)$$

where

$$\begin{aligned} P_B &\equiv \frac{1}{3} (N_B \text{Tr}(\Lambda_B^2) - \text{Tr}(\Lambda_B)^2) - \frac{1}{2} (N_{B+1} \text{Tr}(\Lambda_B^2) + \\ &+ N_B \text{Tr}(\Lambda_{B+1}^2) - 2\text{Tr}(\Lambda_B) \text{Tr}(\Lambda_{B+1})). \end{aligned} \quad (40)$$

Since we shall write the final result as a combination of vacuum expectation values in the Gaussian matrix model, we have chosen to use the usual Vandermonde determinant as the reference measure. Moreover we have not explicitly written $\frac{1}{k^2}$ terms since they do not affect the final result. In fact, they cancel out with the normalization provided by the partition function.

With the help of the expansion (39), it is straightforward to write down the expectation value of the Wilson loop $W^{(A)}$ in terms of P_B and Λ_A . We find

$$\begin{aligned} \langle W^{(A)} \rangle &= N_A + \frac{2}{k} \langle \text{Tr}(\Lambda_A^2) \rangle + \frac{1}{k^2} \left[\frac{2}{3} \langle \text{Tr}(\Lambda_A^4) \rangle + \right. \\ &+ 2 \sum_{B=0}^{2r-1} \left[\langle \text{Tr}(\Lambda_A^2) P_B \rangle - \langle \text{Tr}(\Lambda_A^2) \rangle \langle P_B \rangle \right] \left. \right] + O\left(\frac{1}{k^3}\right), \end{aligned} \quad (41)$$

where all the expectation values in the r.h.s. of eq. (41) are taken in Gaussian matrix model of coupling constant $(-2i\ell_B)$. At the order $\frac{1}{k^2}$ the effect of the interactions is entirely encoded in the combination $\langle \text{Tr}(\Lambda_A^2) P_B \rangle - \langle \text{Tr}(\Lambda_A^2) \rangle \langle P_B \rangle$. However this combination vanishes unless $B = A-1$ or $B = A$ and thus the Wilson loop receives contributions from the nodes $A-1$, A and $A+1$ (we recall that P_B also depends on Λ_{B+1}). This is similar to what occurs in ABJ theories with the difference that the node $A-1$ and $A+1$ are identified there.

Using known results on the expectation values of $\text{Tr}(\Lambda^n)$ and on correlators of traces in the Gaussian matrix model, we finally find

$$\begin{aligned} \frac{\langle W^{(A)} \rangle}{N_A} &= 1 + \frac{i\ell_A N_A}{2k} - \\ &- \frac{1}{24k^2} (4N_A^2 - 3N_{A-1}N_A - 3N_{A+1}N_A - 1) + O\left(\frac{1}{k^3}\right) \end{aligned} \quad (42)$$

This expression coincides with the perturbative result for 1/4 BPS Wilson loop given in (30) dressed with the phase (35) corresponding to framing 1. With the help of cohomological relation (36), we can also build $\langle W_{\psi_i}^{(A)} \rangle$ and we find again the same result (32) of the perturbative computation.

6. Discussion and perspectives

We have studied the two-loop perturbative behavior of the 1/2 BPS Wilson loop operators W_{ψ_1} and W_{ψ_2} introduced in [9,10] in the case of $\mathcal{N} = 4$ Chern–Simons matter quiver theories with alternating levels.

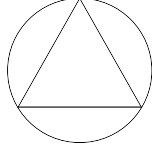


Fig. 2. Example of a three-loop diagram yielding different results for W_{ψ_1} and W_{ψ_2} .

The Feynman diagram analysis of Section 3 has shown that up to two loops the expectation values of W_{ψ_1} and W_{ψ_2} are coincident and match the prediction from the perturbative expansion of the matrix model obtained in Section 4. Remarkably, in the field theory computation the coincidence between the two Wilson loops is true not only for the full result but it holds also for each of the contributing diagrams. At this perturbative order the two Wilson loops share exactly the same properties. We thus have to go up to three loops to look for hints of a possible lifting of the degeneracy between the two classically equivalent 1/2 BPS operators.

Indeed, at three loops some distinctive features in the perturbative computation arise. First of all, at this order the two Wilson loops start giving different results at the level of single diagrams. It is easy to find examples of this behavior and we provide the simplest one in Fig. 2.

Evaluating the diagram for the two Wilson loops we obtain

$$W_{\psi_2} |_{\text{Fig. 2}} = -W_{\psi_1} |_{\text{Fig. 2}} \quad (43)$$

with

$$W_{\psi_1} |_{\text{Fig. 2}} = -\frac{2}{k^3} N_1 N_2 (N_1^2 + N_2^2 + 2) I(\epsilon)$$

$$I(\epsilon) = \frac{4}{3} \Gamma\left(-\frac{1}{2} + 3\epsilon\right) \left[\frac{\Gamma(\frac{1}{2} - \epsilon)\Gamma(1 + \epsilon)}{(4\pi)^{1-\epsilon}\Gamma(1 + 2\epsilon)} \right]^3 \xrightarrow{\epsilon \rightarrow 0} -\frac{1}{24\pi} \quad (44)$$

The extra minus sign in W_{ψ_2} compared to W_{ψ_1} comes from the different scalar couplings in the two Wilson loop definitions. This situation is very similar to what happens for the one-loop fermion exchange contribution of Section 3. However, while in that case the diagram is eventually discarded because the integral has been shown to be $\mathcal{O}(\epsilon)$, in the present case a finite contribution survives in the $\epsilon \rightarrow 0$ limit.

Another source of possible differences might come from the Yukawa vertices in the potential, which start contributing at three loops. In fact, while minimal couplings entering up to two loops are diagonal in the flavor space, Yukawa vertices are in general flavor changing and the computation might become sensible to the flavor choice of the spinor insertions on the contour.

Based on these general observations, we expect a different result for a subset of three-loop Feynman diagrams and it would be crucial to check if the differences are compensated when we sum over all the contributions. If this were the case, the common result

of the two operators should match the three-loop expansion of the matrix model. Instead, if the differences would not cancel against each others, and cannot be absorbed in a change of framing, the prediction from the matrix model could be matched only by a specific linear combination of the two Wilson loops, as suggested in [10]. A more radical possibility is that no linear combination satisfies the constraint and therefore the cohomological equivalence is broken at the quantum level. We will report on the ongoing three-loop analysis in [19].

Moreover, it would be interesting to understand how the W_{ψ_i} operators of the $\mathcal{N} = 4$ models fit in the family of 1/2 BPS Wilson loops recently introduced [20] for general $\mathcal{N} = 2$ theories, where a perturbative analysis such as the one completed in this paper could also be applied.

Acknowledgements

This work has been supported in part by MIUR, INFN and MPNS-COST Action MP1210 “The String Theory Universe”.

References

- [1] J.K. Erickson, G.W. Semenoff, K. Zarembo, Nucl. Phys. B 582 (2000) 155, arXiv: hep-th/0003055.
- [2] N. Drukker, D.J. Gross, J. Math. Phys. 42 (2001) 2896, arXiv:hep-th/0010274.
- [3] V. Pestun, Commun. Math. Phys. 313 (2012) 71, arXiv:0712.2824 [hep-th].
- [4] N. Drukker, S. Giombi, R. Ricci, D. Trancanelli, J. High Energy Phys. 0805 (2008) 017, arXiv:0711.3226 [hep-th].
- [5] A. Kapustin, B. Willett, I. Yaakov, J. High Energy Phys. 1003 (2010) 089, arXiv: 0909.4559 [hep-th].
- [6] N. Drukker, D. Trancanelli, J. High Energy Phys. 1002 (2010) 058, arXiv: 0912.3006 [hep-th].
- [7] V. Cardinali, L. Griguolo, G. Martelloni, D. Seminara, Phys. Lett. B 718 (2012) 615, arXiv:1209.4032 [hep-th].
- [8] N. Drukker, M. Marino, P. Putrov, Commun. Math. Phys. 306 (2011) 511, arXiv: 1007.3837 [hep-th].
- [9] H. Ouyang, J.B. Wu, J.J. Zhang, arXiv:1506.06192 [hep-th].
- [10] M. Cooke, N. Drukker, D. Trancanelli, J. High Energy Phys. 1510 (2015) 140, arXiv:1506.07614 [hep-th].
- [11] D. Gaiotto, E. Witten, J. High Energy Phys. 1006 (2010) 097, arXiv:0804.2907 [hep-th].
- [12] K. Hosomichi, K.M. Lee, S. Lee, S. Lee, J. Park, J. High Energy Phys. 0807 (2008) 091, arXiv:0805.3662 [hep-th].
- [13] M.S. Bianchi, G. Giribet, M. Leoni, S. Penati, J. High Energy Phys. 1310 (2013) 085, arXiv:1307.0786 [hep-th].
- [14] L. Griguolo, G. Martelloni, M. Poggi, D. Seminara, J. High Energy Phys. 1309 (2013) 157, arXiv:1307.0787 [hep-th].
- [15] S.-J. Rey, T. Suyama, S. Yamaguchi, J. High Energy Phys. 0903 (2009) 127, arXiv: 0809.3786 [hep-th].
- [16] M. Mariño, P. Putrov, J. High Energy Phys. 1311 (2013) 199, arXiv:1206.6346 [hep-th].
- [17] H. Ouyang, J.B. Wu, J.J. Zhang, arXiv:1507.00442 [hep-th].
- [18] Y. Imamura, K. Kimura, J. High Energy Phys. 0810 (2008) 040, arXiv:0807.2144 [hep-th].
- [19] M.S. Bianchi, L. Griguolo, M. Leoni, A. Mauri, S. Penati, D. Seminara, in preparation.
- [20] H. Ouyang, J.B. Wu, J.J. Zhang, arXiv:1510.05475 [hep-th].